Int. J. Electrochem. Sci., 6 **(2011)** 2672 - 2687

International Journal of
ELECTROCHEMICAL
SCIENCE
www.electrochemsci.org

Electrochemical Synthesis of Poly(3,4-ethylenedioxythiophene) and Gold Nanocomposite and Its Application for Hypochlorite Sensor

Tsung-Hsuan Tsai, Kuo-Chiang Lin, Shen-Ming Chen[*]

Electroanalysis and Bioelectrochemistry Lab, Department of Chemical Engineering and Biotechnology, National Taipei University of Technology, No.1, Section 3, Chung-Hsiao East Road, Taipei 106, Taiwan (ROC).
[*]E-mail: smchen78@ms15.hinet.net

Received: 5 May 2011 / *Accepted:* 8 June 2011 / *Published:* 1 July 2011

The AuNPs/PEDOT nanocomposite consisting of poly(3,4-ethylendioxythiophene) and Au nanoparticles (AuNPs) can be easily synthesized on electrode surface. It was studied to develop a new NaClO sensor with improved performance with respect to bare electrode and to pure metallic (AuNPs) modified electrodes. This nanocomposite can be performed by electrochemical co-deposition using ionic liquid 1-butyl-3-methylimidazolium tetrafluoroborate (BMT). It was further characterized by surface-confined and linear pH-dependence (-60 mV pH^{-1}) in the electrochemical system. AuNPs/PEDOT exhibits grain-like structure and the significant average diameter between PEDOT and AuNPs, which is due to AuNPs covered over PEDOT surface. The composite of AuNPs/PEDOT was analyzed by XRD and the AuNPs fraction was estimated in 60.29 wt%. The significant electron transfer resistance (R_{et}) is found between PEDOT and AuNPs due to it maintains the partial property of PEDOT and AuNPs. It also exhibits good sensitivity of 208.8 mA M^{-1} cm^{-1} (S/N = 3), detection limit of 1 μM, and linear range of 10^{-6}–9.32×10^{-4} M (correlation coefficient, R^2 = 0.9975) for hypochlorite detection. Moreover, the proposed nanocomposite is suitable to be a hypochlorite sensor and found no interference even in the presence of hydrogen peroxide and ethanol.

Keywords: Poly(3,4-ethylenedioxythiophene), gold nanoparticles, ionic liquids, hypochlorite, electrocatalysis

1. INTRODUCTION

Ionic liquids (ILs) are compounds consisting entirely of ions that exist in liquid state around room temperature. The investigation of ILs has gained increasing attention because of their unique chemical and physical properties such as negligible vapor pressure, low toxicity, wide potential

window, high ionic conductivity and good solubility. ILs had been widely used in extraction (Li et al., 2007) and non-aqueous biocatalysts (Shan et al., 2008). Recently, ILs were also investigated as biocompatible materials for the fabrication of biosensors (Shangguan et al., 2008; Sun et al., 2009; Tu et al., 2009). These researches have confirmed enzyme can maintain high activity and stability in a suitable IL. However, IL lacks enough film forming ability to immobilization enzyme on the electrodes and strongly requires an additional material to aid forming film such as CS (Ragupathy et al., 2009).

Conducting polymer incorporated metallic or semiconducting nanoparticles provides an exciting system and these materials hold potential application in electronics, sensors and catalysis [1–6].

Sensors fabrication based on nanoparticle-incorporated polymeric matrices are of recent technological interest [7, 8]. Metal nanoparticles can be grown inside the polymer matrix by simultaneous electrodepositing of polymer along with metal nanoparticles. Arrays of gold (Au) nanoparticles have been utilized for electrochemical sensors as they exhibit excellent catalytic activity towards various reactions [9-11].

The advantages of electropolymerization are that: (a) thin, uniform and adherent polymer films can be obtained; (b) films can be deposited on a small surface area with a high degree of geometrical conformity and controllable thickness using a specific number of growth cycles in potentiodynamic cycling. Among the numerous polymeric materials developed and studied over the past few decades, polyaniline (PANI), polypyrrole (PPy) and poly (3,4-ethylenedioxythiophene) (PEDOT) constitute an important class [12]. PEDOT has received a significant amount of attention as an electrode material for a variety of applications [13-15]. It shows remarkable stability, provides homogeneous films, and can be synthesized electrochemically from both aqueous and non-aqueous media [16–18]. The conductivity of the PEDOT film does not change significantly with the counter ion [19]. Studies on the behavior of PEDOT in phosphate buffer solutions show a high level of stability when compared to other conducting polymers, suggesting that PEDOT may be a potential candidate for sensor applications and hence it is chosen here for sensing NaClO.

Fabricating sensors based on nanoparticle incorporated/embedded polymeric matrices are of recent technological interest [7,13]. Arrays of Au nanoparticles have been utilized for electrochemical sensors as they exhibit excellent catalytic activity towards various reactions [10, 20–22]. In these, the Au nanoparticles function efficiently as ‘‘electron antennae’’ [23]. Previous work had taken advantage of (a) the hydrophobic/hydrophilic nature of the polymer film; and (b) the signal enhancing character of the embedded Au nanoparticles. Applied a premise that the polymer film contains a distribution of hydrophobic (reduced) and hydrophilic (oxidized) regions [24]. In the present investigation, we attempt to study effect of Au nanoparticles in conjunction with PEDOT with the aim of achieving NaClO determination at low over-potential.

Considering the electrolyte applied in electrochemical system should be eco-friendly. Ionic liquids employed synthesis of nanoparticles emerged as a new interest in the field of green chemistry. Nanostructure materials have been synthesized using ionic liquids as green electrolytes. Such as green synthesis of gold nanoparticles (AuNPs) stabilized by amine-terminated ionic liquid and their electrocatalytic activity in oxygen reduction [25] and green synthesis of highly stable platinum

nanoparticles stabilized by amino-terminated ionic liquid and applied for oxygen reduction and methanol oxidation [26] are few examples. In particular, the chemical and electrochemical synthesis of silver nanostructures using ionic liquids as green electrolytes has been found as interesting one in the green chemistry. Some chemical synthesis of Au and Au nanostructures like nanoparticle, cluster and nanowire formation [27], preparation of AgX (X = Cl, I) nanoparticles using ionic liquids [28], one-step synthesis of conducting polymer–noble metal nanoparticle composites using an ionic liquid [29], ionic liquids of bis(alkylethylenediamine) silver(I)) salts and the formation of silver (0) nanoparticles [30], structure and morphology controllable synthesis of Au/carbon hybrid using ionic liquid as soft-template [31] and partially positively charged silver nanoparticles [32] have been reported.

Hypochlorite is a household cleaning agent and as disinfectant for treatments including drinking water, swimming pool water, treated wastewater for non-potable reuse and others. Normally it is handled as concentrated aqueous solutions and needs periodical control of its concentration to adjust dosages due to the possibility of decomposition (as formula 1). Numbers of methods for hypochlorite determination (e.g. the normalized and well known iodometric titration [33], many colorimetric methods based on reaction of hypochlorite with organic reagents as methyl orange [34], o-tolidine [35], N,N-diethyl-p-phenylenediamine [36,37], thionin [38], 3,3-dimethylnaphtidine [39], and chemiluminiscent methods such as that based on fluorescein test strip [40]). Both some of the reagents and their chloro-derivatives are potential toxic and carcinogenic agents that must be cautiously used.

$$ClO^- \rightarrow Cl^- + 1/2O_2 \qquad (1)$$

It is efficiently catalyzed by several metal oxides as Co_3O_4, NiO, CuO [41], which have been applied to de-chlorination of treated waste water [42, 43]. The analytical usefulness of such heterogeneous catalytic decomposition has been explored in the research by selecting cobalt oxide due to its higher catalytic activity [41].

In this work, we performed AuNPs incorporated PEDOT film on electrode surface and it was used as sensing matrix to determine NaClO. Because the electrocatalytic reduction was seldom to study, we proposed a simple system to prepare AuNPs/PEDOT nanoparticle to electrocatalytically reduce hypochlorite. The proposed nanocomposite was characterized by cyclic voltammetry, atomic force microscopy, scanning electron microscopy, x-ray diffraction, and electrochemical impedance spectrometry to understand its electrochemical behaviors, surface morphology, and composite. It was also studied with the sensitivity and the interference.

2. EXPERIMENTAL

2.1. Reagents

The potassium tetrachloroaurate ($KAuCl_4$, anhydrous, 97%) and 3,4-ethylenedioxythiophene (EDOT) monomer were purchased from Sigma-Aldrich (USA). Ionic liquid 1-butyl-3-methylimidazolium tetrafluoroborate (BMT) (purum > 97 %, HPLC) was purchased from Fluka. All

other chemicals (purchased from Merck) were used of analytical grade (99%). Double distilled deionized water (DDDW) was used to prepare all the solutions. A phosphate buffer solution (PBS) of pH 7.0 was prepared using Na_2HPO_4 (0.05 mol L^{-1}) and NaH_2PO_4 (0.05 mol L^{-1}).

2.2. Apparatus

The CHI 1205a potentiostats (CH Instruments, USA) was applied to perform all electrochemical experiments in this work. The glassy carbon electrode (BAS GCE, d = 0.3 cm; A= 0.07 cm^2, Bioanalytical Systems, Inc., USA) was used as working electrode. The larger electrode (BAS GCE, d = 0.6 cm; A= 0.2826 cm^2) was used for amperometric experiment. A conventional three-electrode system was used in this work and it consists of a reference electrode (Ag/AgCl (KCl_{sat})), a working electrode, and a counter electrode (platinum wire). Particularly, the ionic liquid filled Ag electrodes (Ag/ionic liquid) were used as the reference electrodes when prepared the gold-poly(3,4-ethylenedioxythiophene) film modified electrode. All buffer solutions were entirely altered by deaerating (using nitrogen gas atmosphere). The electrochemical cells were properly sealed to avoid the oxygen interference from the atmosphere. Atomic force microscope (AFM, Model Name: Being Nano-Instruments CSPM-4000, China) was used in tapping mode. Scanning electron microscope (SEM, Model Name: HITACHI S-3000H, Japan) was also used to obtain images of electrode surface. For our convenience, the indium tin oxide (ITO) glass was used as the substrate to immobilize different films for X-ray diffraction (XRD) analysis. Electrochemical impedance spectroscopy (EIS, Model Name: ZAHNER impedance analyzer, Germany) was used to analyze the resistance of electrochemical system.

2.3. Preparation of the modified electrodes including AuNPs/GCE, PEDOT/GCE, and AuNPs/PEDOT/GCE

Prior to the electrochemical deposition process, the glassy carbon electrode (GCE) was well polished by BAS polishing kit with aqueous slurries of alumina powder (0.05 μm). After washing the electrode in double distilled deionized water (DDDW), it was further rinsed and ultra-sonicated to be used.

The gold nanoparticles (AuNPs) modified glassy carbon electrode (AuNPs/GCE) was prepared by adsorption method. The bare electrode was immersed in BMT (pH 1.2) containing 10^{-3} M $KAuCl_4$ for one hour. It was further dried out to be used.

The poly(3,4-ethylenedioxythiophene) film modified glassy carbon electrode (PEDOT/GCE) was prepared by electrochemical method. The bare electrode was immersed in BMT solution (pH 1.2) containing 0.01 M EDOT by cyclic voltammetry (30 scan cycles) from -0.5 to 1.1 V (scan rate = 100 mV s^{-1}).

The gold nanoparticles-poly(3,4-ethylenedioxythiophene) modified glassy carbon electrode (AuNPs/PEDOT/GCE) was also prepared by electrochemical method. The bare electrode was

immersed in BMT (pH 1.2) containing 10^{-3} M $KAuCl_4$ and 0.01 M EDOT by cyclic voltammetry (30 scan cycles) from -0.5 to 1.1 V (scan rate = 100 mV s^{-1})

3. RESULTS AND DISCUSSION

3.1. Electrochemical characteristics of AuNPs/PEDOT electrode

AuNPs/PEDOT nanocomposite was successfully immobilized on electrode surface by a simple method. A cleaned electrode was immersed in the BMT solution (pH 1.2) containing 10^{-3} M $KAuCl_4$ and 0.01 M EDOT by cyclic voltammetry. The cyclic voltammogram (curve a, Fig. 1) of the electrochemical deposition is involving oxidation process of electrode surface [44] and the anodic peak can be observed at 1.1 V. It indicates that PEDOT went firstly to form on electrode surface by oxidation of EDOT monomers. Electrochemical co-deposition might be performed by the interaction between the formed PEDOT and AuNPs. A broadly redox couple was found with an anodic peak of 0.716 V and a cathodic peak of 0.131 V. These redox peaks exhibit more positive potential than that of AuNPs electrode (E_{pa} = 0.670 V, E_{pc} = 0.110 V; as shown in curve b of Fig. 1). The PEDOT is an oxidation state as shown in scheme 1.

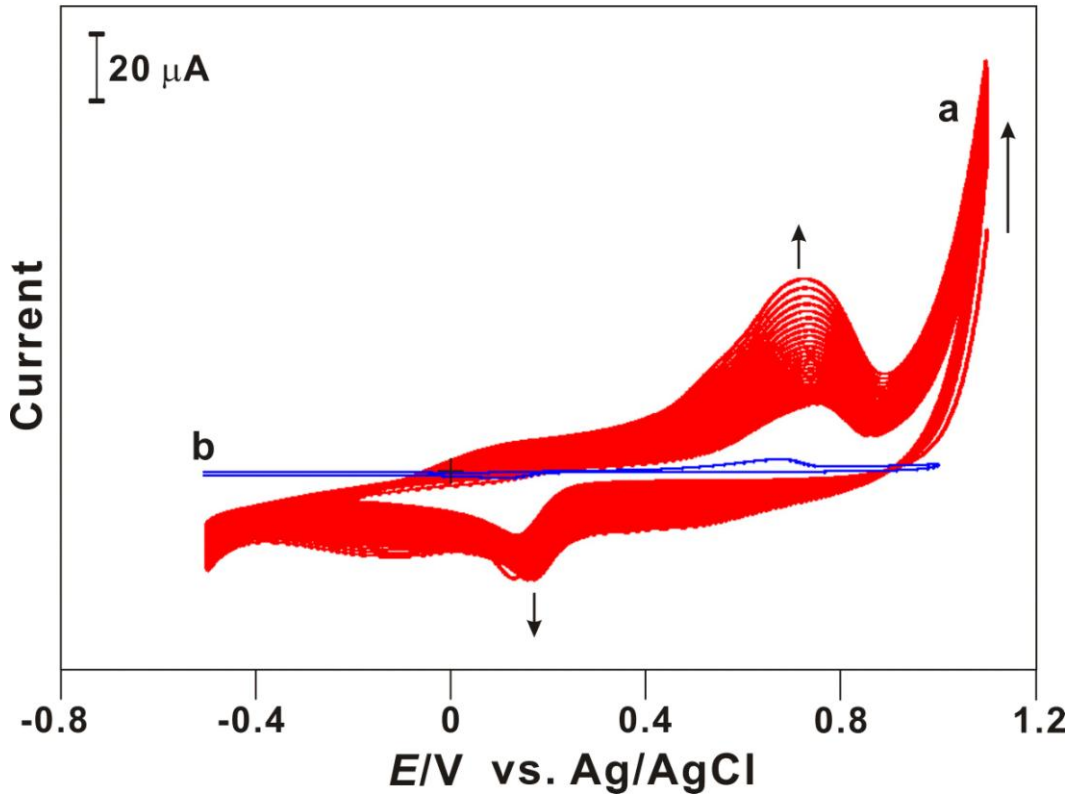

Figure 1. (a) Cyclic voltammograms of the AuNPs/PEDOT preparation using GCE with 30 scan cycles in BMT (pH 1.2) containing 10^{-3} M $KAuCl_4$ and 0.01 M EDOT; and (b) AuNPs/GCE (prepared by adsorption of immersing GCE in BMT containing 10^{-3} M $KAuCl_4$) examined in BMT solution (pH 1.2), scan rate = 0.1 V s^{-1}.

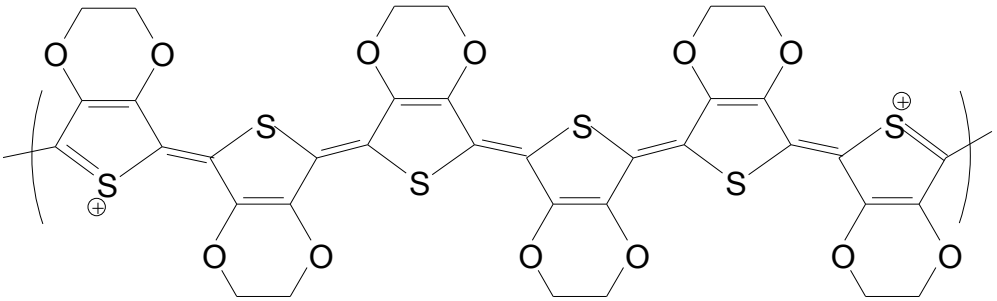

Scheme 1. Oxidation state of PEDOT film.

As previous PEDOT study [45], the gold nanoparticles were incorporated within the polymer backbone through possible gold-sulfur (thiophene) interactions (as shown in Scheme 2). In order to confirm that the AuNPs/PEDOT had been modified on the electrode surface, the voltammogram of PEDOT film was checked and understood that it had almost no redox couple as compared to bare electrode in 0.1 M PBS (pH 7). From Fig. 1, the significant current development of the redox peaks was found similar to AuNPs/GCE. So that we can confirm that the AuNPs/PEDOT film was immobilized on electrode surface by proposed method (electrochemical synthesis). By the way, the construction of conducting polymer/nanoparticles (CP/NPs) was accomplished by the co-deposition of AuNPs incorporated with PEDOT.

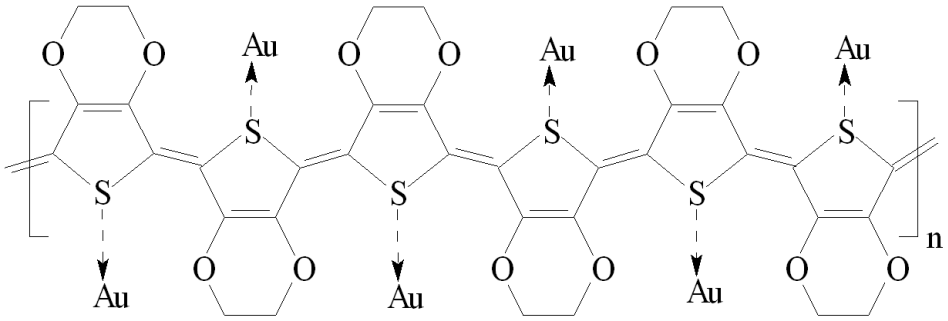

Scheme 2. Structure of AuNPs/PEDOT film.

AuNPs/PEDOT/GCE was electrochemically characterized in various scan rates in PBS solution (pH 7). Fig. 2A shows the cyclic voltammograms of the modified electrode at different scan rates in the scan range of 0.2 – 1.4 V. As increasing the scan rate, AuNPs/PEDOT was found with a broad anodic peak of 1.01 – 1.23 V and a sharp cathodic peak of 0.498 – 0.492 V. Peak current was directly proportional to scan rate up to 1000 mV s^{-1} (as shown in the inset a of Fig. 2A) as expected for surface confined process. The linearity between peak current and scan rate indicates that the electron transfer was very fast and this system was not diffusion control. Logarithmic regressing equation of anodic peak current (I_{pa}) and scan rate (v) can be expressed as $\log(I_{pa})(\mu A) = 0.7375\log(v)(mV\ s^{-1}) - 0.609$, $R^2 = 0.9955$ (as the inset b of Fig. 2A). It was also noticed that the almost straight line of logarithmic

result between anodic current and scan rate. This means that both the current was increasing stably as the increase of scan rate.

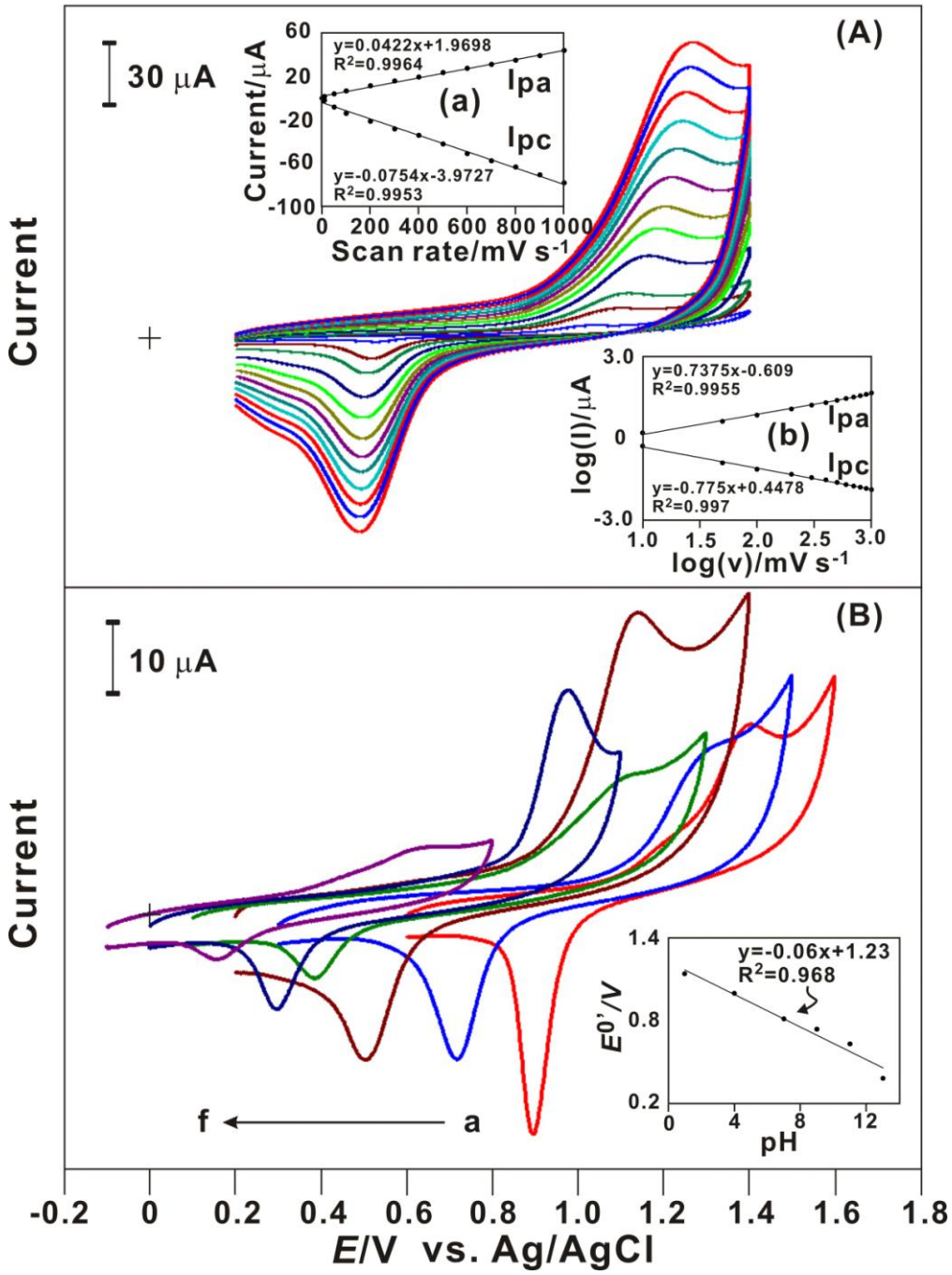

Figure 2. (A) Cyclic voltammograms of AuNPs/PEDOT/GCE examined in 0.1 M PBS (pH 7) with different scan rate from 0.01 to 1 V s^{-1}, respectively. Insets: (a) plot of anodic and cathodic peak current vs. scan rate; (b) plot of logarithm correlation of anodic and cathodic peak current vs. scan rate. (B) Cyclic voltammograms of AuNPs/PEDOT/GCE examined in various pH condition including pH= (a) 1, (b) 4, (c) 7, (d) 9, (e) 11, and (f) 13, respectively, scan rate = 0.1 V s^{-1}. Inset: plot of formal potential ($E^{0'}$) of AuNPs/PEDOT/GCE vs. pH.

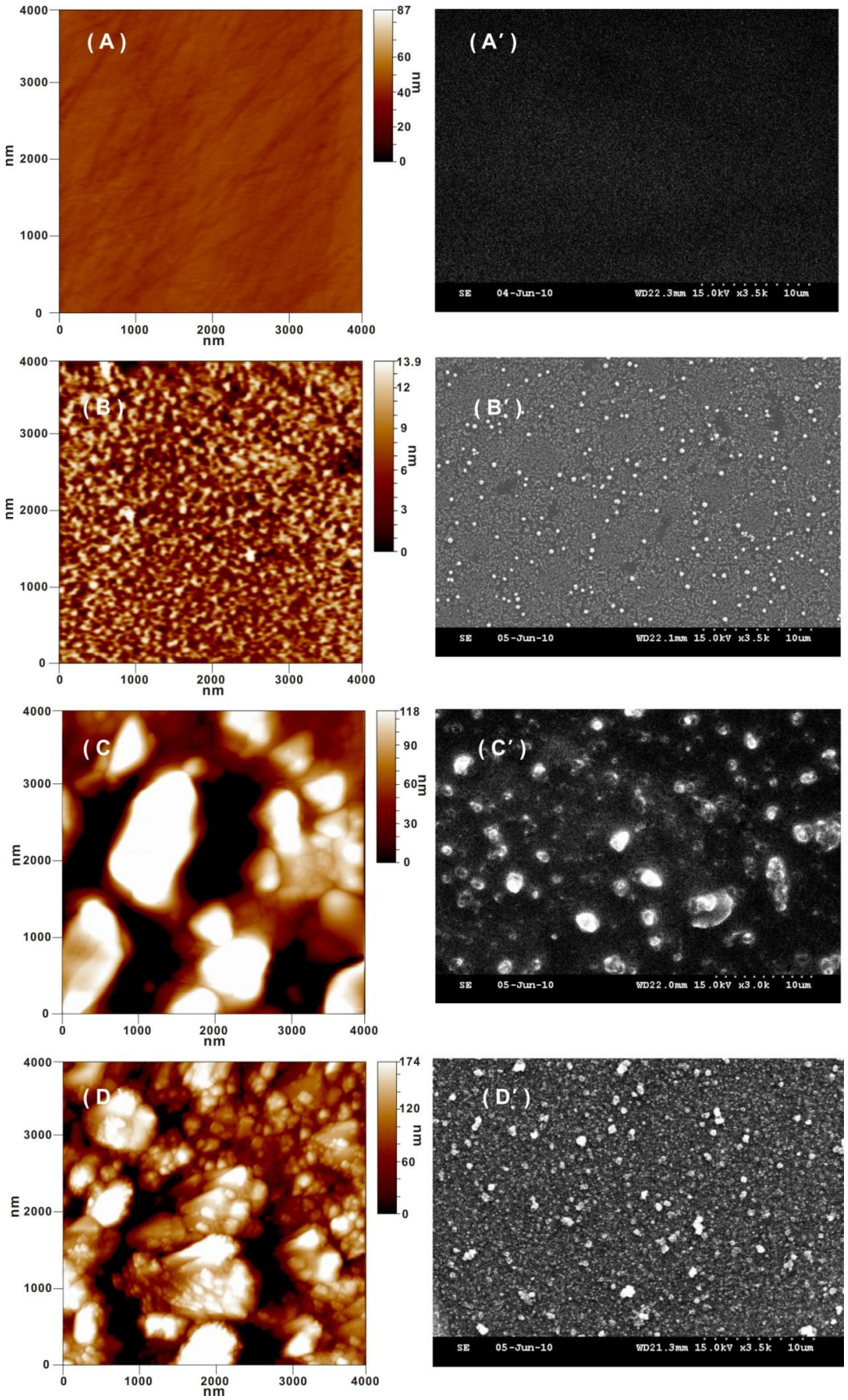

Figure 3. Tapping mode AFM images of (A) bare GCE, (B) AuNPs/GCE, (C) PEDOT/GCE, and (D) AuNPs/PEDOT/GCE; and the SEM images of (A') bare GCE, (B') AuNPs/GCE, (C') PEDO T/GCE, and (D') AuNPs/PEDOT/GCE, respectively.

AuNPs/PEDOT/GCE was also examined in various pH conditions. Fig. 2B displays the pH-dependent voltammetric response of the AuNPs/PEDOT electrode. In order to ascertain this, the voltammetric responses of AuNPs/PEDOT electrode were obtained in the solutions of different pH values varying from 1 to 13. This result demonstrated that the formal potential ($E^{0'}$) of the redox couples were pH dependent and negatively shifted by increasing pH value of the solution. The plot of $E^{0'}$ versus pH yields straight line with a slope of about -60 mV pH^{-1} (as shown in the inset of Fig. 2B). This result was very close to the anticipated Nernstian value of -59 mV pH^{-1} for processes in which equal numbers of electrons and protons were involved in the electrode reactions. The pH dependence suggests that the electroactive sites on the AuNPs/PEDOT electrode behave as true surface active groups influenced by specific solution conditions and not shielded within the electrode interior.

3.2. Morphology studies of AuNPs/PEDOT nanocomposite

Surface morphology of the nanocomposite was studied by AFM and SEM. Fig. 3A-D shows AFM images estimated in the average diameter of 174 nm, 34.5 nm, and 54.9 nm for PEDOT film, AuNPs film, and AuNPs/PEDOT film, respectively. The average diameter of AuNPs/PEDOT was found between PEDOT and AuNPs. In the formation process of AuNPs/PEDOT nanocomposite, PEDOT was firstly performed on electrode surface and further induced gold to form gold-sulfur of the nanocomposite. It means that the average size of AuNPs/PEDOT between AuNPs and PEDOT is extremely like AuNPs covered over PEDOT of AuNPs/PEDOT nanocomposite. The partial weight of AuNPs and PEDOT was estimated with average thickness ($t_{Au} = 9.7\times10^{-9}$ cm, $t_{PEDOT} = 8.23\times10^{-8}$ cm), density ($\rho_{Au} = 19.32$ g/cm^3, $\rho_{PEDOT} = 1.5$ g/cm^3 [46]), and occupied area ($A_{Au} = 0.07$ cm^2, $A_{PEDOT} = 0.07$ cm^2). We had calculated the partial weight of 13.12 ng and 8.64 ng for AuNPs and PEDOT, respectively. So the partial fraction of AuNPs was evaluated by 60.29 wt% ($w_{Au}/(w_{Au} + w_{PEDOT})$) in the nanocomposite.

3.3. XRD analysis of AuNPs/PEDOT nanocomposite

Fig. 4 shows the XRD result of AuNPs/PEDOT nanocomposite prepared by the proposed method. The diffraction features were found at 2 theta as 35.19°, 38.20°, 43.47°, 44.65°, 50.63°, and 56.28°. These patterns corresponded to Au(222), Au(111), Au(331), Au(420), Au(422), and Au(511) planes of the standard cubic phase of Au, respectively. Some peaks were found in 14.69° and 21.34° for PEDOT. And the others were found in 30.30°, 60.05°, and 72.44° for the ITO substrate. The elements of AuNPs/PEDOT nanocomposite were known by the XRD result.

3.4. EIS analysis of AuNPs/PEDOT nanocomposite

Electrochemistry impedance spectroscopy (EIS) technique is an effective method to probe the features of surface modified electrodes. From the shape of an impedance spectrum, the electron-transfer kinetics and diffusion characteristics can be extracted. The respective semicircle parameters

correspond to the electron transfer resistance (R_{et}) and the double layer capacity (C_{dl}) nature of the modified electrodes.

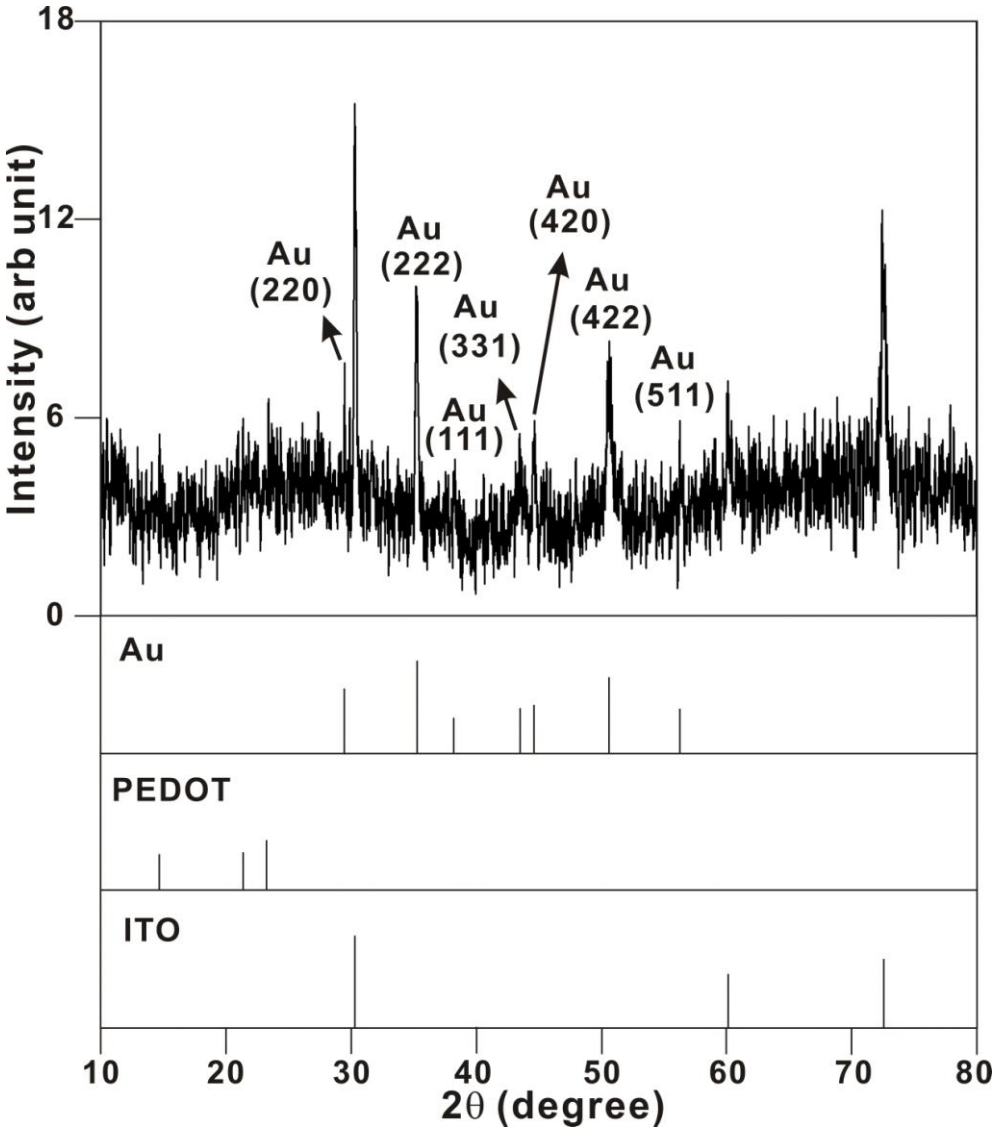

Figure 4. X-ray diffraction patterns of AuNPs/PEDOT film modified on ITO glass substrate.

The electrochemical activity of AuNPs/PEDOT modified GCE was examined using EIS technique. Fig. 5A shows the Nyquist plots for bare GCE, AuNPs/GCE, PEDOT/GCE, and AuNPs/PEDOT/GCE, respectively. As compared to bare GCE (R_{et} = 1154 Ω, Fig. 5A(d)), these film modified electrodes show the smaller semicircle parameters. These modified electrodes obtained the R_{et} of 72.39 Ω, 188.35 Ω, and 479.36 Ω for PEDOT/GCE (Fig. 5A(a)), AuNPs/PEDOT/GCE (Fig. 5A(b)), and AuNPs/GCE (Fig. 5A(c)), respectively. PEDOT/GCE was found an almost straight line (Fig. 5A(a)) with a very small depressed semicircle arc (R_{et} = 72.39 Ω) which means that the PEDOT accelerates the electron transfer rate and provides a network structure to disperse nano-gold particles. Moreover, it was noticed that the R_{et} might be lowered by PEDOT in the electrochemical system.

Particularly, the AuNPs/PEDOT/GCE has the R_{et} value between PEDOT and AuNPs. It means that the AuNPs/PEDOT nanocomposite maintains the partial nature of AuNPs and PEDOT due to the composite distribution. It can be concluded that PEDOT not only can help the co-deposition of AuNPs but also can lower the R_{et} in the electrochemical system.

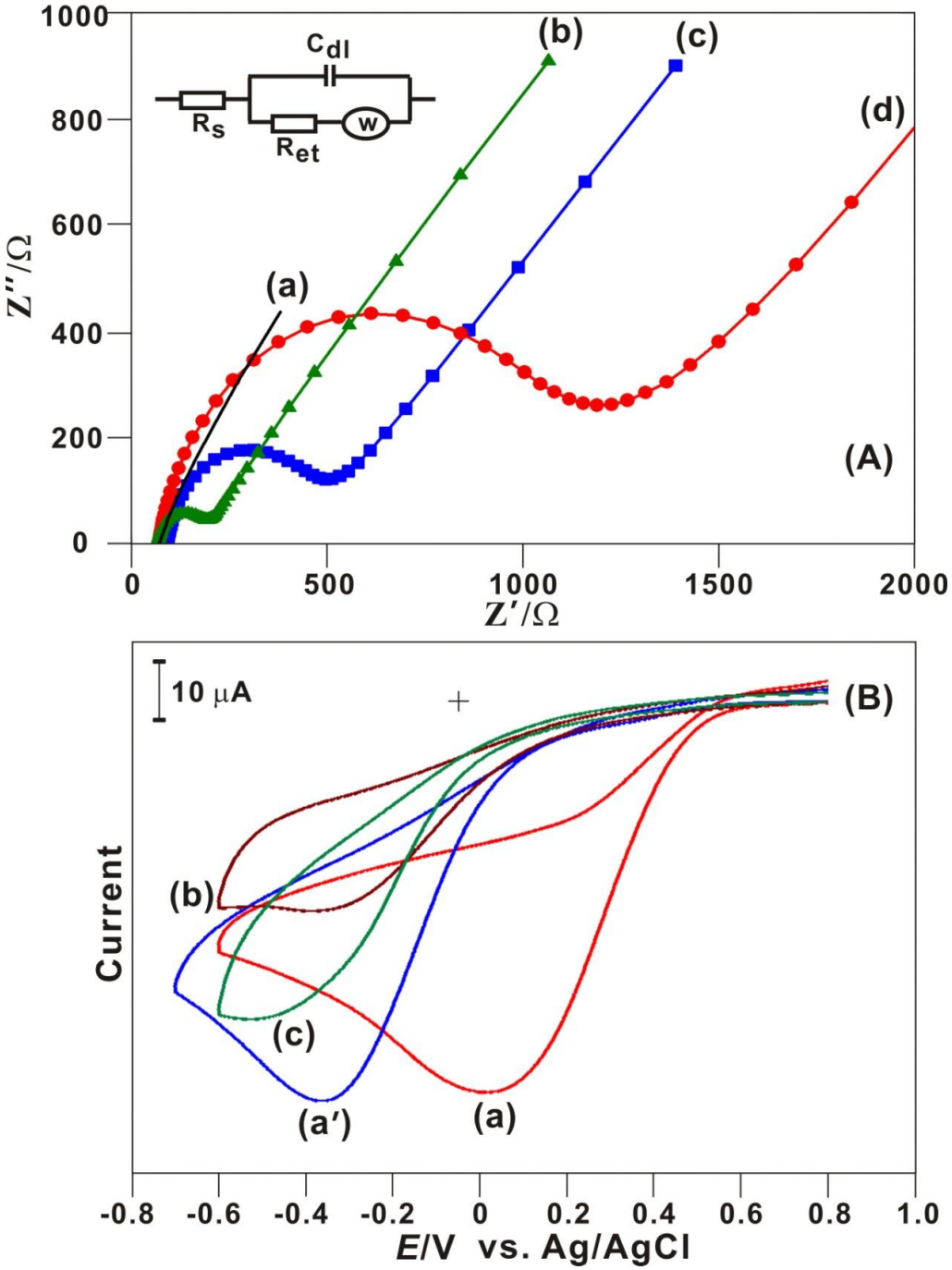

Figure 5. (A) Electrochemical impedance spectra of (a) PEDOT/GCE, (b) AuNPs/PEDOT/GCE, (c) AuNPs/GCE, and (d) bare GCE examined in 0.1 M PBS (pH 7). (B) Cyclic voltammograms of (a) AuNPs/PEDOT/GCE, (b) PEDOT/GCE, (c) AuNPs/GCE, and (a') bare GCE examined in 0.1 M PBS (pH 7) containing 10^{-4} M NaClO, scan rate = 0.1 V s^{-1}. All tests were carried out in the absence of oxygen.

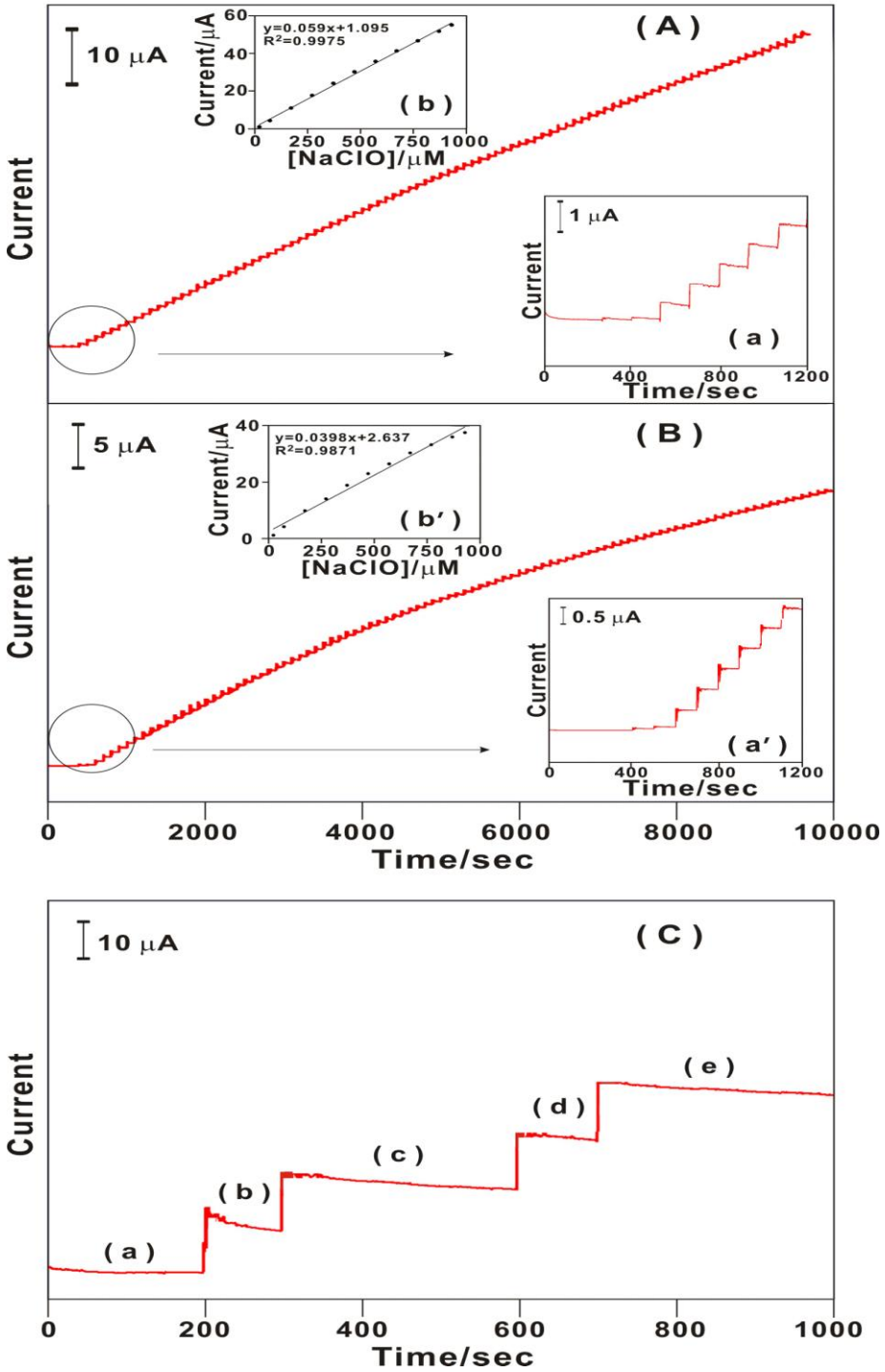

Figure 6. Amperometric responses of AuNPs/PEDOT/GCE in 0.1 M PBS (pH 7) with sequential additions of (A) standard NaClO and (B) real NaClO sample, respectively (Rotating speed = 1000 rpm, Eapp. = 0 V; Insets: (a) & (a') are scale-up of current response for (A) standard NaClO and (B) real NaClO during 0–1200 s; (b) & (b') are plot of concentration vs. catalytic current for (A) standard NaClO and (B) real NaClO during 0–1200 s). (C) Amperometric responses of AuNPs/PEDOT/GCE examined in 0.1 M PBS (pH 7) containing (a) 0 (blank), (b) 1×10^{-5} M NaClO, (c) 2×10^{-5} M NaClO + 1×10^{-5} M H_2O_2 + 1×10^{-5} M C_2H_5OH, (d) 3×10^{-5} M NaClO + 1×10^{-5} M H_2O_2 + 1×10^{-5} M C_2H_5OH, and (e) 4×10^{-5} M NaClO + 1×10^{-5} M H_2O_2 + 1×10^{-5} M C_2H_5OH, respectively (Rotating speed = 1000 rpm, Eapp. = 0 V). All tests were carried out in the absence of oxygen

3.5. Electrocatalysis studies of hypochlorite

Fig. 5B shows cyclic voltammograms of electrocatalytic reduction of hypochlorite performed by (a) AuNPs/PEDOT/GCE, (b) PEDOT/GCE, (c) AuNPs/GCE, and (a') bare GCE, respectively. By comparison, AuNPs/PEDOT/GCE shows higher current response and a lower over-potential of approximate 0 V. As expected in CP/NPs construction, the conducting polymer lowers over-potential and the nanoparticles enhance the electrocatalytic current. In this case, the concept was accomplished by that the activation energy of hypochlorite is lowered by PEDOT while electrocatalytic current enhanced by AuNPs. From the result, AuNPs/PEDOT nanocomposite is one good material to develop hypochlorite sensor.

3.6. Amperometric response of hypochlorite electrocatalysis by AuNPs/PEDOT nanocomposite

It was carried out using amperometric technique in order to assure that the catalytic reduction of hypochlorite at AuNPs/PEDOT modified electrode in stirred solutions ($E_{app.}$ = 0 V).

Table 1. Comparison of sensing abilities for hypochlorite determination with different electrodes.

Electrodes	Analytes	$E_{app.}$ (V vs. Ag/AgCl)	Reaction	LOD[d] (M)	LCR[e] (M)	Sensitivity (mA M^{-1} cm^{-2})	Ref.
AChE[a]/ISFET	$HOCl/OCl^-$	---	---	1×10^{-5}	1×10^{-5}-3×10^{-4}	---	[47]
BDD[b] electrode	Cl	1.4	Oxidation	---	5.6×10^{-4}-2.8×10^{-3}	264	[48]
BDD[b] electrode	Cl	1.4	Oxidation	2.3×10^{-7}	2.8×10^{-6}-5.6×10^{-5}	---	[48]
Pt, Au, GC electrode	Cl	1.1	Oxidation	2.8×10^{-5}	1.1×10^{-4}-1.1×10^{-2}	---	[49]
Cobalt oxide electrode	Cl_2	---	Oxidation	1.4×10^{-4}	1×10^{-3}-6×10^{-3}	---	[50]
Pt, Pt oxide electrode	Cl	---	Oxidation	1.1×10^{-4}	2.8×10^{-3}-1.1×10^{-2}	---	[51]
Gold thin-film microelectrode	Cl	0.35	Oxidation	5.6×10^{-7}	5.6×10^{-6}-1.4×10^{-5}	504	[52]
CNT/epoxy resin	Cl	-0.1	Reduction	5.6×10^{-7}	5.6×10^{-7}-1.1×10^{-4}	18.5	[53]
Rhodamine/FP[c]	HOCl	---	---	3×10^{-7}	5×10^{-7}-7×10^{-6}	---	[54]
Nano Au-PEDOT/GCE	HOCl	0	Reduction	1×10^{-6}	1×10^{-6}-9.32×10^{-4}	208.8	This Work

[a] Acetylcholinesterase; [b] Boron-doped diamond; [c] Rhodamine spiroring-based fluorescent probe; [d] LOD = limit of detection; [e] LCR = linear

Fig. 6A & B shows amperometric response of AuNPs/PEDOT/GCE for standard NaClO (Fig. 6A) and real NaClO sample (Fig. 6B), respectively. In the period of 400–4000 s, the current response was directly proportional to hypochlorite concentration as shown in the inset (b) & (b') of Fig. 6.

In the detection of standard NaClO (as shown in Fig. 6A), a linear dynamic range was found of 1–932 μM (correlation coefficient, R^2 = 0.9975). The detection limit and the sensitivity was found of 1 μM and 208.8 mA M^{-1} cm^{-2} (signal-to-noise ratio, S/N = 3), respectively. It had fast response (response time = 5 s) and good reproducibility (3.7%, n=6). The reproducibility was evaluated from the slope of

three calibration plots performed with different modified electrodes. In the detection of real sample (as shown Fig. 6B), it had the sensitivity of 170.9 mA M^{-1} cm^{-2} and the linear dynamic range of 1–472 μM (I_{pc}(μA) = 0.0483C_{NaClO}(μM) + 0.8216, R^2 = 0.996, S/N = 3).

These results were comparable to those already reported determination of hypochlorite at different modified electrodes, for example, enzyme potentiometric sensor for hypochlorite species detection [47]. As compared with IC, LC, LC-MS, and HPLC, the electroanalysis method has competitive superiority due to low cost, fast analysis, and low detection limit. By comparison (as shown in Table 1), the AuNPs/PEDOT nanocomposite is one good material for hypochlorite determination. The OSHA (Occupation Safety and Health Administration, USA) claimed the highest allowable peak concentration (5 minute exposure for five minutes in a 4-hour period) is 200 ppm (part per million) for NaClO, the detection limit of 1 μM translating to 0.0744 ppm (1 μM NaClO = 74.4 g/mole×1 μ mole/L = 74.4 1 μg/L = 0.0744 mg/L = 0.0744 ppm) is much less than the OSHA allowance. Therefore, A

uNPs/PEDOT is really suitable to develop a NaClO sensor.

3.7. Interference studies

Amperometric response of AuNPs/PEDOT/GCE was monitored in 0.1 M PBS (pH 7) containing hypochlorite, hydrogen peroxide, and ethanol ($E_{app.}$ = 0 V; rotation speed = 1000 rpm). Fig. 6C shows the current response for (a) blank, (b) 1×10^{-5} M NaClO, (c) 2×10^{-5} M NaClO + 1×10^{-5} M H_2O_2 + 1×10^{-5} M C_2H_5OH, (d) 3×10^{-5} M NaClO + 1×10^{-5} M H_2O_2 + 1×10^{-5} M C_2H_5OH, and (e) 4×10^{-5} M NaClO + 1×10^{-5} M H_2O_2 + 1×10^{-5} M C_2H_5OH, respectively. The background signal of proposed film was initially checked and obtained in the blank (as Fig. 6C(a)). It was found the almost flat current stage during 0–200 s. As first addition of 1×10^{-5} M NaClO in the 200^{th} s, the current response was raising immediately to form the plateau current (as Fig. 6C(b)). The current response increased only for NaClO even in the presence of 1×10^{-5} M NaClO, 1×10^{-5} M H_2O_2, and 1×10^{-5} M C_2H_5OH (as Fig. 6C(c)). Furthermore, it was found the similar phenomenon in the 600^{th} and 700^{th} s (as shown in Fig. 6C (d) & (e)). As the result, AuNPs/PEDOT/GCE exhibits good amperometric response for hypochlorite determination without interference even in the presence of hydrogen peroxide and ethanol.

4. CONCLUSIONS

Here we report an electrochemical method to form stable AuNPs/PEDOT nanoparticle (using ionic liquid (BMT) as green electrolytes) on electrode surface. The electrochemical synthesized nanocomposite has been characterized by surface-confined, pH dependence, gold fraction, element composite, and specific electron transfer resistance. The nanocomposite can provide competitive sensitivity for the determination of hypochlorite. Furthermore, it is found no interference even in the presence of hydrogen peroxide and ethanol.

ACKNOWLEDGEMENTS
This work was supported by NSC (National Science Council), Taiwan.

References

1. K.M. Kost, D.E. Bartak, B. Kazee, T. Kuwana, *Anal. Chem.* 60 (1988) 2379-2384.
2. A.Kitani, T. Akashi, K. Sugimoto, S. Ito, *Synth. Met.* 121 (2001) 1301-1302.
3. W.-H. Kao, T. Kuwana, *J. Am. Chem. Soc.* 106 (1984) 473-476.
4. F. Ficicioglu, F. Kadirgan, *J. Electroanal. Chem.* 430 (1997) 179-182.
5. A.Drelinkiewicz, M. Hasik, M. Kloc, *Catal. Letters* 64 (2000) 41-47.
6. E.T. Kang, Y.P. Ting, K.G. Neoh, K.L. Tan, *Synth. Met.* 69 (1995) 477-478.
7. C.R. Raj, T. Okajima, T. Ohsaka, *J. Electroanal. Chem.* 543 (2003) 127-133.
8. R. Gangopadhyay, A. De, *Chem. Mater.* 12 (2000) 608-622.
9. A.Doron, E. Katz, I. Willner, *Langmuir* 11 (1995) 1313-1317.
10. A.N. Shipway, E. Katz, I. Willner, *Chem. Phys. Chem.* 1 (2000) 18-52.
11. A.B. Moghaddam, T. Nazari, J. Badraghi, M. Kazemzad, *Int. J. Electrochem. Sci.* 4 (2009) 247-257.
12. H.B. Mark, N. Atta, K.L. Petticrew, H. Zimmer, Y. Shi, S.K. Lunsford, J.F. Rubinson, A. Galal, *Bioelectrochem. Bioenerg.* 38 (1995) 229-245.
13. K. Krishnamoorthy, R.S. Gokhale, A.Q. Contractor, A. Kumar, *Chem. Commun.* (2004) 820-821.
14. H. Yamato, M. Ohwa, W. Wernet, *J. Electroanal. Chem.* 397 (1995) 163-170.
15. M. Behpour, S.M. Ghoreishi, E. Honarmand, *Int. J. Electrochem. Sci.* 5 (2010) 1922-1933.
16. A.Sakmeche, J.J. Aaron, M. Fall, A. Aeiyach, M. Jouini, J.C. Lacroix, P.C. Lacaze, *Chem. Commun.* (1996) 2723-2724.
17. V.S. Vasantha, K.L.N. Phani, *J. Electroanal. Chem.* 520 (2002) 79-88.
18. M. Dietrich, J. Heinze, G. Heywang, F. Jonas, *J. Electroanal. Chem.* 369 (1994) 87-92.
19. L.B. Groenendaal, G. Zotti, P.-H. Aubert, S.M. Waybright, J.R. Reynolds, *Adv. Mater.* 15 (2003) 855-879.
20. M. Haruta, M. Date, *Appl. Catal. A* 222 (2001) 42.
21. S.G. Penn, L. Hey, M.J. Natan, *Curr. Opin. Chem. Biol.* 7 (2003) 609-615.
22. P. Alivisatos, *Nat. Biotechnol.* 22 (2004) 47-52.
23. K.R. Brown, A.P. Fox, M.J. Natan, *J. Am. Chem. Soc.* 118 (1996) 1154-1157.
24. C.R. Martin, L.S. Van Dyke, in: R.W. Murray (Ed.), *Molecular Design of Electrode Surfaces*, Wiley, New York, 1992, pp. 403–424.
25. Z. Wang, Q. Zhang, D. Kuehner, A. Ivaska, L. Niu, *Green Chem.* 10 (2008) 907-909.
26. F. Li, F. Li, J. Song, J.F. Song, D. Han, L. Niu, *Electrochem. Commun.* 11 (2009) 351-354.
27. A.I. Bhatt, A. Mechler, L.L. Martin, A.M. Bond, *J. Mater. Chem.* 17 (2007) 2241-2250.
28. E. Rodil, L. Aldous, C. Hardacre, M.C. Lagunas, *Nanotechnology* 19 (2008) 105603.
29. J.M. Pringle, O.W. Jensen, C. Lynam, G.G. Wallace, M. Forsyth, D.R. MacFarlane, *Adv. Funct. Mater.* 18 (2008) 2031-2040.
30. M. Iida, C. Baba, M. Inoue, H. Yoshida, E. Taguchi, H. Furusho, *Chem. Eur. J.* 14 (2008) 5047-5056.
31. S.Y. Wu, Y.S. Ding, X.M. Zhang, H.O. Tang, L. Chen, *J. Solid State Chem.* 181 (2008) 2171-2177.
32. S.W. Kang, K.Char, Y.S. Kang, *Chem. Mater.* 20 (2008) 1308-1311.
33. APHA, AWWA, WPCF, *in Metodos Normalizados para el Analisis de Aguas Potables y Residuals*, Diaz de Santos, Madrid, 1992, pp. 55–61.
34. D.J. Leggett, N.H. Chen, D.S. Mahadevappa, *Analyst* 107 (1982) 433-441.

35. J.G. March, M. Gual, B.M. Simonet, *Talanta* 58 (2002) 995-1001.
36. L. Moberg, B. Karlberg, *Anal. Chim. Acta* 407 (2000) 127-133.
37. A.Chaurasia, K.K. Verma, *Fresenius J. Anal. Chem.* 351 (1995) 335-337.
38. B. Narayana, M. Mathew, K. Vipin, N.V. Sreekumar, T. Cherian, *J. Anal. Chem.* 60 (2005) 706-709.
39. J. Ballesta-Claver, M.C. Valencia-Miron, L.F. Capit´an-Vallvey, *Anal. Chim. Acta* 522 (2004) 267-273.
40. E. Pobozy, K. Pyrzynska, B. Szostek, M. Trojanowicz, *Microchem. J.* 51 (1995) 379-386.
41. A.Hamano, Y. Suenaga, *Kayaku Gakkaishi* 55 (1994) 58-61.
42. V.S. Londhe, P.R. Kamath, *Water Res.* 9 (1975) 1009-1010.
43. *Japan Patent* 56108587.
44. S. Thiagarajan, T.H. Tsai, S.M. Chen, *Biosens. Bioelectronics* 24 (2009) 2712–2715.
45. S. Vinod Selvaganesh, J. Mathiyarasu, K. L. N. Phani, V. Yegnaraman, *Nanoscale Res. Lett.* 2 (2007) 546-549
46. S.C. Luo, E.M. Ali, N.C. Tansil, H.H. Yu, S. Gao, E.A.B. Kantchev, J.Y. Ying, *Langmuir* 24 (2008) 8071-8077.
47. A.P. Soldatkin, D.V. Gorchkov, C. Martelet, N. Jaffrezic-Renault, *Sens. Actuators B* 43 (1997) 99–104.
48. M. Murata, T.A. Ivandini, M. Shibata, S. Nomura, A. Fujishima, Y. Einaga, *J. Electroanal. Chem.* 612 (2008) 29-36.
49. F. Kodera, M. Umeda, A.Yamada, *Anal. Chimi. Acta* 537 (2005) 293-298.
50. J.G. March, B.M. Simonet, *Talanta* 73 (2007) 232.
51. F. Kodera, M. Umedab, A. Yamada, *Electrochim. Acta* 53 (2008) 7961.
52. R. Olive-Monllau, J. Orozco, C. Fernandez-Sanchez, M. Baeza, J. Bartroli, C. Jimenez-Jorquera, F. Cespedes, *Talanta* 77 (2009) 1739
53. R. Olive-Monllau, A. Pereira, J. Bartroli, M. Baeza, F. Cespedes, *Talanta* 81 (2010) 1593.
54. X.Q. Zhan, J.H. Yan, J.H. Su, Y.C. Wang, J. He, S.Y. Wang, H. Zheng, J.G. Xu, *Sens. Actuators B*, doi:10.1016/j.snb.2010.07.057.